



HAL
open science

The Type IX Secretion System and Its Role in Bacterial Function and Pathogenesis

P.D. Veith, M.D. Glew, D.G. Gorasia, E.C. Reynolds, E. Cascales

► **To cite this version:**

P.D. Veith, M.D. Glew, D.G. Gorasia, E.C. Reynolds, E. Cascales. The Type IX Secretion System and Its Role in Bacterial Function and Pathogenesis. *Journal of Dental Research*, 2022, 101 (4), pp.374-383. 10.1177/00220345211051599 . hal-03654995

HAL Id: hal-03654995

<https://amu.hal.science/hal-03654995>

Submitted on 29 Apr 2022

HAL is a multi-disciplinary open access archive for the deposit and dissemination of scientific research documents, whether they are published or not. The documents may come from teaching and research institutions in France or abroad, or from public or private research centers.

L'archive ouverte pluridisciplinaire **HAL**, est destinée au dépôt et à la diffusion de documents scientifiques de niveau recherche, publiés ou non, émanant des établissements d'enseignement et de recherche français ou étrangers, des laboratoires publics ou privés.

Revised Ms JDR-21-1000

The Type IX Secretion System and its Role in Bacterial Function and Pathogenesis

P.D. Veith¹, M.D. Glew¹, D.G. Gorasia¹, E. Cascales² and E.C. Reynolds^{1*}

¹ Oral Health CRC, Melbourne Dental School, Bio21 Institute, The University of Melbourne, Victoria, 3010, Australia.

² Laboratoire d'Ingénierie des Systèmes Macromoléculaires (LISM), Institut de Microbiologie, Bioénergies and Biotechnologie (IM2B), Aix-Marseille Université, Centre National de la Recherche Scientifique (CNRS), UMR7255, 31 Chemin Joseph Aiguier CS7071, 13009 Marseille Cedex 20, France.

*Corresponding author: e.reynolds@unimelb.edu.au

Abstract word count: 279

Total words (Abstract to Acknowledgments): 4,318

Total number of tables/figures: 5

Number of references: 60

Keywords

Periodontal disease(s)/periodontitis; Bacterial virulence; Host pathogen interactions; Ultrastructure; Microbiology

ABSTRACT (300 word limit)

Porphyromonas, *Tannerella* and *Prevotella* species found in severe periodontitis use the Type IX Secretion System (T9SS) to load their outer membrane surface with an array of virulence factors. These virulence factors are then released on outer membrane vesicles (OMVs) which penetrate the host to dysregulate the immune response to establish a positive feedback loop of chronic, inflammatory destruction of the tooth's supporting tissues. In this review we present the latest information on the molecular architecture of the T9SS and provide mechanistic insight into its role in secretion and attachment of cargo proteins to produce a virulence coat on cells and OMVs. The recent molecular structures of the T9SS motor comprising PorL and PorM as well as the secretion pore Sov, together with advances in the overall interactome have provided insight into the possible mechanisms of secretion. We propose the presence of PorL/M motors arranged in a circle at the inner membrane with bent periplasmic rotors interacting with the PorN protein. At the outer membrane, we envisage a slide carousel model where the PorN protein is driven around a circular track composed of PorK. Cargo proteins are transported by PorN to PorW and the Sov translocon just as slides are rotated to the projection window. Secreted proteins are proposed to then be shuttled along highways consisting of the PorV shuttle protein to an array of attachment complexes distributed around the cell. The cell surface attachment of cargo is a hallmark of the T9SS and in *Porphyromonas gingivalis* and *Tannerella forsythia*, this attachment is achieved via covalent bonding to a linking sugar synthesised by the Wbp/Vim pathway. The cell-surface attached cargo are enriched on OMVs which are then released from the cell.

Severe Periodontitis: A T9SS driven dysbiosis?

Periodontitis is a prevalent, chronic inflammatory disease associated with a dysbiotic subgingival plaque that results in the destruction of the tooth's supporting tissues. The global prevalence of severe periodontitis has been estimated at 11.2% and the disease is ranked the 6th most prevalent disease worldwide (Tonetti et al. 2017). The economic burden of periodontitis in the US and Europe has been estimated as US\$342 billion (Botelho et al. 2021). Over the last 15 years evidence has accumulated that periodontitis is linked with a range of systemic diseases like diabetes, cardiovascular diseases, certain cancers and dementia, suggesting that periodontal health is vital for good general health (Hajishengallis and Chavakis 2021).

1
2
3 The identification of bacterial species that characterize a subgingival plaque dysbiotic
4 signature started with the seminal cross-sectional study by Socransky *et al* (1998). This study
5 was the first to show a close association of a specific bacterial consortium with severe
6 periodontitis (Socransky et al. 1998). The consortium comprising *Porphyromonas gingivalis*,
7 *Treponema denticola* and *Tannerella forsythia* was referred to as the red complex as these
8 species were found together in deep periodontal pockets and they were the only bacteria of
9 the 40 bacterial taxa studied that closely associated with disease.
10
11

12
13
14
15
16 The technology for identification of bacterial species in dental plaque has progressed
17 significantly since these earlier studies such that now using Next-Generation Sequencing
18 (NGS) techniques over 200 different taxa can be identified in the microbial community of a
19 plaque sample. There are now many cross-sectional plaque microbiome studies published
20 comparing periodontal health with disease using NGS. These microbiome studies have
21 identified bacterial species that seem preferentially associated with health or disease, and
22 largely they have confirmed the close association of the red complex bacteria in deep
23 periodontal pockets from patients with severe periodontitis where these three species *P.*
24 *gingivalis*, *T. denticola* and *T. forsythia* can be found in abundance within a complex
25 microbial community (Kirst et al. 2015; Lenartova et al. 2021; Shi et al. 2020).
26
27
28
29
30
31
32
33

34 A limitation with cross-sectional analyses of subgingival plaque samples is the dynamic
35 nature of periodontitis where sites may be inactive at any single sampling time hence
36 prospective clinical studies are required to better link the microbial composition with disease
37 progression. One prospective study by Byrne *et al* (2009) was designed to determine the level
38 of certain bacterial species in subgingival plaque of patients with moderate to severe
39 periodontitis at three monthly intervals during a maintenance program (Byrne et al. 2009).
40 The levels of these species at sites that progressed by losing 2 mm or greater clinical
41 attachment could then be compared with their levels at sites that remained stable. This study
42 confirmed the finding that the red complex bacteria were strongly associated with disease
43 severity but importantly extended the finding by showing that the emergence of these
44 pathogens, particularly *P. gingivalis* preceded attachment loss, implying a direct link with
45 disease progression. In fact, the study showed that the level of *P. gingivalis* was an excellent
46 biomarker for disease progression at severe periodontitis sites.
47
48
49
50
51
52
53
54
55

56
57 These pathogenic species associated with severe periodontitis display mutualistic
58 symbioses in metabolism, growth and biofilm formation as well as synergistic virulence in
59
60

1
2
3 animal models of infection (Tan et al. 2014). In fact, animal model studies have shown that *P.*
4 *gingivalis* can drive dysbiosis and that the proteases called gingipains are the major virulence
5 factors of the bacterium. These studies have resulted in *P. gingivalis* being referred to as a
6 keystone pathogen in periodontitis (Hajishengallis et al. 2012). Further evidence of the
7 importance of these bacterial species in severe disease is their temporospatial relationship in
8 the periodontal pocket. Studies investigating the architecture and temporospatial distribution
9 of pathogens in subgingival plaque have demonstrated that species from the genera
10 *Porphyromonas*, *Tannerella*, *Prevotella* and *Treponema* (e.g. *P. gingivalis*, *T. forsythia*,
11 *Prevotella intermedia* and *T. denticola*) are found at the base of deep pockets in severe
12 periodontitis patients and therefore are referred to as site specialists (Kigure et al. 1995; Mark
13 Welch et al. 2019). Metagenomic analyses of these bacteria demonstrates an expanded
14 functionality or over-representation of genes encoding proteases, adhesins, iron acquisition
15 systems and secretion systems. In fact, it has been suggested that even though the
16 microbiomes of severe periodontitis sites may be taxonomically heterogeneous they are
17 functionally congruent through the expression and secretion of functionally similar virulence
18 factors (Altabtbaei et al. 2021; Shi et al. 2020). Interestingly a common characteristic of *P.*
19 *gingivalis*, *T. forsythia* and *P. intermedia* is the newly identified T9SS which these species use
20 to load their cell surface with an array of virulence factors including proteases, adhesins,
21 haemolysins and internalins (Veith et al. 2017). **These virulence factors are actively released**
22 **on outer membrane vesicles (OMVs) which can then penetrate the pocket epithelium to**
23 **dysregulate the host defenses (O'Brien-Simpson et al. 2009). The best example of this process**
24 **is the secretion of the major virulence factors of *P. gingivalis*, the gingipains, by the T9SS.**
25
26
27
28
29
30
31
32
33
34
35
36
37
38
39
40
41
42
43

44 **The T9SS loads the outer membrane with virulence factors for a mobilised vesicle army**

45
46 The T9SS is a nanomachine that secretes cargo proteins from the periplasm to the cell surface
47 of Gram-negative bacteria. The T9SS is not ubiquitous and is restricted to species belonging
48 to the *Bacteroidetes-Chlorobi-Fibrobacteres* superphylum. All T9SS cargo proteins are
49 translocated across the inner membrane (IM) by the Sec translocon due to their N-terminal
50 signal sequence and are then recruited by the T9SS for secretion across the outer membrane
51 (OM) by their structurally conserved C-terminal domain (CTD) sequence (Lasica et al. 2017;
52 Veith et al. 2017). The cargo proteins are then attached to the cell surface via covalent
53 linkage to A-LPS to form a virulence coat, surrounding both cells and released OMVs. The
54
55
56
57
58
59
60

genes required for these processes fall into two broad groups (Table 1). The first group of genes code for components of the T9SS machinery, including IM proteins (PorL and PorM), OM associated proteins (PorE, PorF, PorG, PorK, PorN, PorP, PorQ, PorT, PorU, PorV, PorW, PorZ and Sov) (Naito et al. 2019; Sato et al. 2010) and components involved in signal transduction and gene regulation (PorA, PorX, PorY and SigP) (Yukitake et al. 2020).

Besides PorA, all of these proteins have orthologs in *T. forsythia* and *P. intermedia* (Table 1). Deletion of these genes prevents the secretion, maturation and attachment of cargo to the cell surface resulting in non-pigmented colonies of *P. gingivalis* on a blood agar plate (Sato et al. 2010).

The second group include genes involved in the biosynthesis of A-LPS. The polysaccharide portion of A-LPS is proposed to consist of an anionic phosphorylated branched mannan (Paramonov et al. 2015), however accumulating evidence suggests that A-LPS includes a more conventional polysaccharide requiring four glycosyltransferases specific for A-LPS (WbaP, GtfC, VimF and GtfF) and two further glycosyltransferases (GtfE and GtfB) which are also required for the synthesis of O-polysaccharide in "O-LPS" (Shoji et al. 2018). The novel A-LPS linking sugar which is bonded to the cargo proteins was recently identified to be an 2-N-seryl-3-N-acetylglucuronamide in *P. gingivalis* and 2-N-glycyl-3-N-acetylmannuronic acid in *T. forsythia* that is synthesized by the novel Wbp/Vim pathway comprising WbpA, UgdA, WbpB, WbpE [also known as PorR], WbpD, WbpS, VimE and VimA (Veith et al. 2020). Deletion of A-LPS biosynthetic genes results in loss of surface attachment, with the cargo released into the growth medium (Gorasia et al. 2015) and non-pigmented colonies on blood agar (Shoji et al. 2018). *P. intermedia* does not have orthologs for several enzymes in the Wbp/Vim pathway (Table 1) suggesting it may utilize a different type of linking sugar to attach its cargo to the cell surface.

Since T9SS cargo proteins are greatly enriched in *P. gingivalis* OMVs and comprise approximately 60% of the protein content (Veith et al. 2014; Veith et al. 2018), OMVs can be considered an extension of the T9SS, delivering cargo into the periodontal tissues. OMVs play important roles in adaptation to stress, biofilm formation, host immunomodulation, and adherence to host cells and dysbiosis (Cecil et al. 2019; Veith et al. 2018; Zhang et al. 2020). There are many mechanisms by which OMVs are generated involving peptidoglycan biosynthesis, envelope stress response, nutrient response such as to iron-limitation, regulation of OM proteins binding to peptidoglycan and regulation of the VacJ/Yrb phospholipid (PL) import system (Roier et al. 2016; Schwechheimer and Kuehn 2015; Zhang et al. 2020).

1
2
3
4
5
6
7
8
9
10
11
12
13
14
15
16
17
18
19
20
21
22
23
24
25
26
27
P. gingivalis uses its T9SS to secrete and anchor many characterized virulence proteins to the surface of the cell as recently reviewed (Lasica et al. 2017; Veith et al. 2017). Some of these virulence proteins are discussed below and include the abundant cysteine proteases known as gingipains (Kgp, RgpA, RgpB) which are the bacterium's major virulence factors that degrade host proteins and extract peptides for growth. The gingipains also play a major role in disease pathogenesis through dysregulation of host defense and inflammatory responses (Guo et al. 2010). Other proteases are PepK, CPG70, PrtT and periodontain. Peptidylarginine deiminase (PPAD) is linked to rheumatoid arthritis (Gully et al. 2014). PG0350 and PG1374 are leucine-rich repeat containing proteins with homology to internalin J from *Listeria monocytogenes* and may facilitate invasion of host cells and affect mono- and heterotypic-species biofilm formation. Mfa5 is one of three ancillary tip proteins essential for assembly of the tip fimbrellins of Mfa1 fimbriae. **The T9SS and Mfa5 in particular have been shown to be essential for the recently discovered "surface translocation" of *P. gingivalis* (Moradali et al. 2019).**

28
29
30
31
32
33
34
35
36
37
38
39
40
41
42
43
44
45
P. gingivalis is auxotrophic for heme and the acquisition of iron plays an essential role in its growth and virulence (Smalley and Olczak 2017). The availability of iron in the host is extremely low due to strong sequestration by host hemin binding proteins such as the haemoglobin-haptoglobin complex, hemopexin and albumin, therefore *P. gingivalis* has evolved very efficient systems for the extraction, capture and transportation of heme (Rangarajan et al. 2017; Smalley and Olczak 2017). An additional role of the gingipains is the extraction of heme from host proteins, converting it to the black pigmented heme dimer, μ -oxo bisheme, and efficiently storing it on the cell surface bound to A-LPS. *P. gingivalis* has a 10-fold greater specific hemin binding affinity and greater heme storage capacity than the accessory pathogen *P. intermedia* (Socransky et al. 1998; Tompkins et al. 1997).

46
47
48
49
50
51
52
53
54
55
56
57
58
59
60
Recently, we have shown that A-LPS can be exchanged between different *P. gingivalis* cells through close contact or through fusion with OMVs with the potential for transfer of the bound μ -oxo bisheme (Glew et al. 2021). This has important consequences in terms of altering the oral microbiota and may help explain why *P. gingivalis* has such a key role in pathogenesis (Hajishengallis et al. 2012). The T9SS by loading OMVs with μ -oxo bisheme can enable *P. gingivalis* to affect the availability of iron for other periodontitis-related bacterial species that require hemin for growth. Thus, LPS-hemin exchange with *P. gingivalis*, particularly with its OMVs, may contribute to polymicrobial synergy in the development of a dysbiotic community.

1
2
3
4
5
6
7
8
9
10
11
12
13
14
15
16
17
18
19
20
21
22
23
24
25
26
27
28
29
30
31
32
33
34
35
36
37
38
39
40
41
42
43
44
45
46
47
48
49
50
51
52
53
54
55
56
57
58
59
60

Transposon sequencing (TnSeq) technology has enabled the genome-wide determination of *P. gingivalis* essential genes for growth and fitness. These strategies have compared the populations of saturated transposon mutagenized genes before and after planktonic growth in rich medium (Hutcherson et al. 2016; Klein et al. 2012), after colonisation of oral epithelial cells (TIGK), after infection in a murine abscess model (Miller et al. 2017) or after exposure to cigarette smoke extract (Hutcherson et al. 2020). Essential genes for growth are “inherently essential” and cannot be considered for assessment for fitness in defined environments which are “conditionally essential”. **Table 1** summarises the *P. gingivalis* TnSeq data for T9SS-related genes that are inherently essential or required for fitness under three conditions. Sixty-five percent of the T9SS components and 58% of the genes specific for the biosynthesis of A-LPS were found to be essential for growth. In contrast, only 23% of T9SS cargo genes were inherently essential but 77% were required for fitness under one to three conditions (**Table 1**). These TnSeq analyses show an important difference between T9SS component and cargo protein genes. The majority of T9SS components are essential for growth but the majority of the T9SS cargo proteins are important for fitness which exemplifies the importance of the T9SS-related genes for *P. gingivalis* survival and fitness. It also reinforces our understanding of the T9SS cargo proteins as important virulence factors.

The T9SS Nanomachine: Molecular architecture and function

A fully assembled T9SS has not been isolated yet, suggesting it is a dynamic system. Nevertheless, full or partial structures and functions of many components have been elucidated. Structures of major sub-complexes including the motor complex and the translocon have been solved using cryo-electron microscopy (cryo-EM), and protein interactome studies are helping to form a cohesive functional picture of the T9SS as a whole as detailed below.

The T9SS translocon

The identity of the components that form the OM translocon was unknown until recently. Sov/SprA, a 267 kDa, protein was hypothesized to form the secretion channel in the OM based on its large size and its retention in a minimal T9SS found in some members of the *Bacteroidetes* phylum (Lauber et al. 2018). Accordingly, these authors tagged and isolated

1
2
3 SprA containing complexes from *Flavobacterium johnsoniae* and solved their structures by
4 cryo-EM. Two complexes were solved, one with SprA bound to the PorV OM β -barrel
5 protein and the other with SprA bound to the Plug protein (Lauber et al. 2018). SprA forms
6 an extremely large, 36-stranded transmembrane β -barrel with an external cap, a lateral
7 opening above the membrane and an internal solvent-filled pore of approximately 70 Å, large
8 enough to allow the secretion of folded cargo proteins. This is the largest single polypeptide
9 transmembrane β -barrel identified to date. When bound to PorV, the lateral opening of SprA
10 faces the extracellular loops of PorV, while in the Plug-SprA complex, the lateral opening is
11 free, but the periplasmic entrance is blocked by the Plug protein. The authors proposed a
12 model for the T9SS translocon mechanism whereby the two ends of the channel are
13 alternately gated. In this model, the SprA-PorV complex represents the “open-state” and
14 allows uptake of the T9SS substrates from the periplasm while the SprA-Plug complex
15 represents the state after the T9SS substrates have been released, leading to unidirectional
16 transport of substrates through the translocon.
17
18
19
20
21
22
23
24
25
26
27
28
29

30 *The shuttle protein*

31
32 The most abundant T9SS component is PorV, also called LptO, a 14-stranded OM β -barrel
33 protein related to the family of FadL transporters (Chen et al. 2011; Gorasia et al. 2020b). As
34 mentioned above, PorV associates with the T9SS translocon and additionally, PorV binds to
35 T9SS substrates harboring a CTD signal (Glew et al. 2017). Given that the only known
36 similarity amongst the T9SS cargo is the presence of the CTD signal, it was suggested that
37 PorV binds to the CTD signal enabling it to collect substrates from the translocon and shuttle
38 them to the attachment complexes (discussed below) (Glew et al. 2017). This theory was
39 elegantly supported by the work of Lauber *et al*, where a long extracellular loop of PorV was
40 found to penetrate inside the lumen of the SprA pore (Lauber et al. 2018) suggesting PorV
41 collects the T9SS substrates directly from the translocon. However, it is unclear whether
42 substrate bound PorV moves through the OM to reach an attachment complex or whether the
43 T9SS substrate gets passed along a chain of PorV molecules on the cell surface.
44
45
46
47
48
49
50
51
52
53
54
55

56 *The attachment complex*

57
58 Most of the T9SS cargo proteins in *P. gingivalis* are attached to the cell surface. It is known
59 that T9SS substrates are modified with A-LPS explaining cell attachment, however the exact
60

1
2
3 mechanism of how this occurred was unclear until recently. The 440 kDa attachment
4 complex, comprising the PorU and PorZ surface proteins and the PorV and PorQ OM β -
5 barrels, was identified using blue native gel electrophoresis (Glew et al. 2017). Both PorU
6 and PorZ possess a CTD signal and utilize the T9SS to reach the cell surface. However,
7 rather than being processed and conjugated to A-LPS (Glew et al. 2012; Lasica et al. 2016),
8 PorU and PorZ are anchored to the OM through their binding to PorV and PorQ respectively
9 (Glew et al. 2017). The crystal structure of PorZ showed that it consists of two beta-propeller
10 domains in addition to its CTD (Lasica et al. 2016). The proposed function of PorZ was to
11 bind carbohydrate/A-LPS (Glew et al. 2017; Lasica et al. 2016) which was confirmed by
12 detecting the specific binding of recombinant PorZ to A-LPS (Madej et al. 2021).
13 Furthermore, PorZ interacts with PorU in an A-LPS-dependent manner supporting a role for
14 PorZ in presenting the A-LPS substrate to PorU (Madej et al. 2021). The catalytic component
15 of the attachment system, PorU uses a sortase-like mechanism to cleave the CTD signal at the
16 cell surface, and covalently attach the A-LPS linking sugar (see above) to the new C-terminus
17 of the cargo proteins via a peptide bond (Glew et al. 2012; Gorasia et al. 2015; Veith et al.
18 2020). This results in permanent anchorage of the T9SS substrates to the cell surface.
19
20
21
22
23
24
25
26
27
28
29
30
31
32

33 *The proposed T9SS powertrain*

34
35 PorK, PorL, PorM and PorN together form a trans-envelope complex (Sato et al. 2010;
36 Vincent et al. 2017) which appears to be anchored to the peptidoglycan layer via the PorP-
37 PorE complex (Gorasia et al. 2020a; Gorasia et al. 2020c). The PorP component was shown
38 to interact with the trans-envelope complex (Vincent et al. 2017), while PorE was shown to
39 associate with the peptidoglycan (Trinh et al. 2020). Cryo-EM analysis of a purified complex
40 containing PorK, PorN and PorG showed that these three proteins form large 50 nm ring-like
41 structures (Gorasia et al. 2016). Biochemical evidence suggested that the PorK/N ring was
42 localised in the periplasm and tethered to the OM, a location supported by recent *in-situ*
43 images from cryo-EM (Gorasia et al. 2020a). Although the PorK/N ring and PorL/M motor
44 are purified as separate complexes, PorM is known to interact with the ring proteins (Vincent
45 et al. 2017).
46
47
48
49
50
51
52
53
54

55 The structure of the molecular motor that drives secretion and gliding motility was
56 solved by cryo-EM and found to be composed of a PorL pentamer associated with a PorM
57 dimer. In total, ten α -helices from PorL form the 'stator' which is membrane-embedded and
58
59
60

1
2
3 surrounds the two trans-membrane helices of the PorM ‘rotor’ and causes them to rotate by
4 using energy from the proton motive force (Hennell James et al. 2021). The periplasmic
5 domains of PorM form a bent shaft which traverses the periplasm and at the tip is calculated
6 to rotate around a circle of 18 nm where it may drive processes at the OM through its contact
7 with the PorK/N rings (Hennell James et al. 2021; Sato et al. 2020). The *porKLMN*
8 transcription unit is well conserved amongst bacteria which use the T9SS supporting the
9 proposed flow of energy from the motor complex to the PorK/N ring.
10
11
12
13
14

15
16 While the motor has five subunits of PorL and two subunits of PorM, the PorK/N ring
17 has 32-36 subunits of each component (Gorasia et al. 2016). Given the relative whole cell
18 abundance of these proteins is approximately 1 PorK to 3 PorL to 1 PorM to 1PorN (Glew et
19 al. 2017; Gorasia et al. 2020b), there is likely to be a ring of motors directly underneath the
20 PorK/N ring to form a symmetrical funnel-shaped cage in the periplasm (Fig. 1).
21
22
23
24

25 Until recently, the Sov translocon had no known connection to the PorKLMN system, such
26 that the pathway of energy provision for secretion was unclear. Recently we provided
27 evidence that PorW connects these two disparate complexes in *P. gingivalis* and have now
28 confirmed direct interactions between PorW and PorN and also between PorW and Sov
29 (Gorasia et al. 2020a); (Gorasia and Lunar Silva *et al.* unpublished). For the first time these
30 interactions map out a potential pathway for energy transduction to the Sov translocon.
31 Additionally, this same interactome maps out a pathway for the delivery of cargo to the
32 translocon since the CTD signal of multiple cargo proteins have been shown to interact with
33 PorM, PorN and PorW (Vincent et al. 2018); (Lunar Silva *et al.* unpublished).
34
35
36
37
38
39
40

41 The emerging design suggests that cargo proteins are recruited by the rotating PorM
42 shaft and transferred to PorN. PorN may in turn be physically moved around the fixed
43 circular track composed of PorK and deliver the cargo to PorW, like slides are delivered to
44 the projection window in a slide carousel. PorW would then transfer the cargo to the secretion
45 pore Sov (Fig. 2). This design enables cargo to be recruited from a large catchment volume
46 and be delivered to the secretion pore in potentially high concentrations. This concentration
47 effect alone may be the “energy transduction” that drives secretion, or else PorN may
48 additionally transfer mechanical energy through its interaction with PorW. This scheme may
49 also accommodate gliding motility which has been shown to use a helical track along which
50 motility adhesins flow (Nakane et al. 2013). To convert the circular track into a helical one it
51 may be sufficient just to add an additional component to the track. The gliding-specific GldJ
52 lipoprotein which shares homology with GldK/PorK is a perfect candidate for this role and
53
54
55
56
57
58
59
60

1
2
3 has already been suggested to form the helical track in *F. johnsoniae* (Braun and McBride
4
5 2005).
6
7
8

9 **Formation of the virulence coat**

10
11 An intriguing and unique element of the T9SS is the attachment of numerous cargo proteins
12 to the cell surface via A-LPS to produce a ‘virulence coat’ around the cell. We initially
13 thought that both the translocon and the attachment complexes would be located within the
14 PorK/N rings, which would make the work of the PorV shuttle protein more efficient by
15 limiting its distance of diffusion (Gorasia et al. 2020a). However, with the PorK/N rings
16 implicated in energy transduction and substrate delivery, the barrier theory is no longer
17 required to explain their function. Furthermore, it is known that PorV and other attachment
18 complex members are highly enriched in OMVs, whereas PorK, PorN, PorW and Sov are not
19 (Veith et al. 2014), and therefore for the barrier theory to be correct, OMVs would need to be
20 formed preferentially from the OM immediately above and inside the PorK/N rings, which
21 we have found no evidence for and seems unlikely. It is likely then, that Sov together with
22 PorV and the attachment system are located outside the PorK/N rings (Fig. 1, Fig. 2).
23 Furthermore, we have developed a mechanistic model for the cargo shuttle process which
24 greatly extends the cell surface area serviced by the attachment system (Fig. 3). The PorV
25 barrels are proposed to interact laterally to form branching chains that interconnect each Sov
26 translocon with multiple attachment complexes. The cargo proteins are passed along the
27 PorV chains until they reach an attachment complex where they are anchored to A-LPS and
28 released (Fig. 3). The basis for this idea is three-fold. Firstly, lateral interactions between OM
29 β -barrels is common, for example in porin trimers in other species (Ma et al. 2018) and in the
30 RagAB peptide transporter of *P. gingivalis* (Madej et al. 2020) making the idea of lateral
31 interactions between adjacent PorV molecules plausible. Secondly, lateral interactions
32 involving PorV are already known to occur for the Sov-PorV complex (Lauber et al. 2018)
33 and lateral interactions between PorV and PorQ in the attachment complexes also seem likely
34 to help hold the complexes together. And thirdly, passing substrates along a PorV chain
35 obviates the need for an unlikely bi-directional highway of PorV molecules diffusing through
36 the membrane to load and off-load the cargo. **Our model also considers the relative whole cell
37 stoichiometry recently shown to be approximately 1 PorK/N ring to 8 attachment complexes
38 to 100 PorV molecules (Glew et al. 2017; Gorasia et al. 2020b).**
39
40
41
42
43
44
45
46
47
48
49
50
51
52
53
54
55
56
57
58
59
60

CONCLUSION

The dynamic nature of periodontitis can be explained by the temporospatial emergence of periodontal pathogens at the base of a periodontal pocket. These pathogens secrete virulence factors using the T9SS and then release them into host tissue on OMVs to dysregulate the immune defense to generate a destructive, chronic, inflammatory response in a positive feedback loop to progress disease (Fig 4). The mechanisms by which the T9SS loads virulence factors onto the surface of cells and OMVs appears to involve a novel circular conveyor belt to deliver energy and cargo proteins (virulence factors) from the motor to the secretion pore and then to the surface for attachment.

ACKNOWLEDGEMENTS

This work was supported by the Australian National Health and Medical Research Council grants ID 1123866 and 1193647 and the Australian Research Council grant DP200100914.

AUTHOR CONTRIBUTIONS

P.D.Veith, contributed to conception and design, contributed to acquisition, analysis, and interpretation, drafted manuscript, critically revised manuscript; M.D. Glew, contributed to conception and design, contributed to acquisition, analysis, and interpretation, drafted manuscript, critically revised manuscript; D.G. Gorasia, contributed to conception and design, contributed to acquisition, analysis, and interpretation, drafted manuscript, critically revised manuscript; E. Cascales, contributed to acquisition, analysis, and interpretation, critically revised manuscript; E.C. Reynolds, contributed to conception and design, contributed to acquisition, analysis, and interpretation, drafted manuscript, critically revised manuscript. All authors gave final approval and agree to be accountable for all aspects of the work.

DECLARATION OF CONFLICTING INTERESTS

1
2
3 The authors declared no potential conflicts of interest with respect to the research, authorship,
4 and/or publication of this article.
5
6
7
8
9
10
11
12
13
14
15
16
17
18
19
20
21
22
23
24
25
26
27
28
29
30
31
32
33
34
35
36
37
38
39
40
41
42
43
44
45
46
47
48
49
50
51
52
53
54
55
56
57
58
59
60

For Peer Review

REFERENCES

- Altabtbaei K, Maney P, Ganesan SM, Dabdoub SM, Nagaraja HN, Kumar PS. 2021. Anna Karenina and the subgingival microbiome associated with periodontitis. *Microbiome*. 9(1):97.
- Botelho J, Machado V, Leira Y, Proenca L, Chambrone L, Mendes JJ. 2021. Economic burden of periodontitis in the United States and Europe - an updated estimation. *J Periodontol*. 10.1002/JPER.21-0111.
- Braun TF, McBride MJ. 2005. *Flavobacterium johnsoniae* GldJ is a lipoprotein that is required for gliding motility. *J Bacteriol*. 187(8):2628-2637.
- Byrne SJ, Dashper SG, Darby IB, Adams GG, Hoffmann B, Reynolds EC. 2009. Progression of chronic periodontitis can be predicted by the levels of *Porphyromonas gingivalis* and *Treponema denticola* in subgingival plaque. *Oral Microbiol Immunol*. 24(6):469-477.
- Cecil JD, Sirisaengtaksin N, O'Brien-Simpson NM, Krachler AM. 2019. Outer membrane vesicle-host cell interactions. *Microbiol Spectr*. 7(1).
- Chavent M, Duncan AL, Rassam P, Birkholz O, Helie J, Reddy T, Beliaev D, Hambly B, Piehler J, Kleanthous C, et al. 2018. How nanoscale protein interactions determine the mesoscale dynamic organisation of bacterial outer membrane proteins. *Nat Commun*. 9(1):2846.
- Chen YY, Peng B, Yang Q, Glew MD, Veith PD, Cross KJ, Goldie KN, Chen D, O'Brien-Simpson N, Dashper SG, et al. 2011. The outer membrane protein LptO is essential for the O-deacylation of LPS and the co-ordinated secretion and attachment of A-LPS and CTD proteins in *Porphyromonas gingivalis*. *Mol Microbiol*. 79(5):1380-1401.

- 1
2
3 Glew MD, Veith PD, Peng B, Chen YY, Gorasia DG, Yang Q, Slakeski N, Chen D, Moore
4
5 C, Crawford S, et al. 2012. PG0026 is the C-terminal signal peptidase of a novel
6
7 secretion system of *Porphyromonas gingivalis*. J Biol Chem. 287(29):24605-24617.
8
9
10 Glew MD, Veith PD, Chen D, Gorasia DG, Peng B, Reynolds EC. 2017. PorV is an outer
11
12 membrane shuttle protein for the type IX secretion system. Sci Rep. 7(1):8790.
13
14
15 Glew MD, Gorasia DG, McMillan PJ, Butler CA, Veith PD, Reynolds EC. 2021.
16
17 Complementation *in trans* of *Porphyromonas gingivalis* lipopolysaccharide
18
19 biosynthetic mutants demonstrates lipopolysaccharide exchange. J Bacteriol.
20
21 203:e00631-00620.
22
23
24 Gorasia DG, Veith PD, Chen D, Seers CA, Mitchell HA, Chen YY, Glew MD, Dashper SG,
25
26 Reynolds EC. 2015. *Porphyromonas gingivalis* type IX secretion substrates are
27
28 cleaved and modified by a sortase-like mechanism. PLoS Pathog. 11(9):e1005152.
29
30
31 Gorasia DG, Veith PD, Hanssen EG, Glew MD, Sato K, Yukitake H, Nakayama K, Reynolds
32
33 EC. 2016. Structural insights into the PorK and PorN components of the
34
35 *Porphyromonas gingivalis* type IX secretion system. PLoS Pathog. 12(8):e1005820.
36
37
38 Gorasia DG, Chreifi G, Seers CA, Butler CA, Heath JE, Glew MD, McBride MJ,
39
40 Subramanian P, Kjaer A, Jensen GJ, et al. 2020a. *In situ* structure and organisation of
41
42 the type IX secretion system. bioRxiv.2020.2005.2013.094771.
43
44
45 Gorasia DG, Glew MD, Veith PD, Reynolds EC. 2020b. Quantitative proteomic analysis of
46
47 the type IX secretion system mutants in *Porphyromonas gingivalis*. Mol Oral
48
49 Microbiol. 35(2):78-84.
50
51
52 Gorasia DG, Veith PD, Reynolds EC. 2020c. The type IX secretion system: Advances in
53
54 structure, function and organisation. Microorganisms. 8(8):1173.
55
56
57 Gully N, Bright R, Marino V, Marchant C, Cantley M, Haynes D, Butler C, Dashper S,
58
59 Reynolds E, Bartold M. 2014. *Porphyromonas gingivalis* peptidylarginine deiminase,
60

- 1
2
3 a key contributor in the pathogenesis of experimental periodontal disease and
4
5 experimental arthritis. PLoS One. 9(6):e100838.
6
7
8 Guo Y, Nguyen KA, Potempa J. 2010. Dichotomy of gingipains action as virulence factors:
9
10 from cleaving substrates with the precision of a surgeon's knife to a meat chopper-like
11
12 brutal degradation of proteins. Periodontol 2000. 54(1):15-44.
13
14
15 Hajishengallis G, Darveau RP, Curtis MA. 2012. The keystone-pathogen hypothesis. Nat Rev
16
17 Microbiol. 10(10):717-725.
18
19
20 Hajishengallis G, Chavakis T. 2021. Local and systemic mechanisms linking periodontal
21
22 disease and inflammatory comorbidities. Nat Rev Immunol. 21(7):426-440.
23
24
25 Hennell James R, Deme JC, Kjr A, Alcock F, Silale A, Lauber F, Johnson S, Berks BC, Lea
26
27 SM. 2021. Structure and mechanism of the proton-driven motor that powers type 9
28
29 secretion and gliding motility. Nat Microbiol. 6(2):221-233.
30
31
32 Hutcherson JA, Gogeneni H, Yoder-Himes D, Hendrickson EL, Hackett M, Whiteley M,
33
34 Lamont RJ, Scott DA. 2016. Comparison of inherently essential genes of
35
36 *Porphyromonas gingivalis* identified in two transposon-sequencing libraries. Mol
37
38 Oral Microbiol. 31(4):354-364.
39
40
41 Hutcherson JA, Gogenini H, Lamont GJ, Miller DP, Nowakowska Z, Lasica AM, Liu C,
42
43 Potempa J, Lamont RJ, Yoder-Himes D, et al. 2020. *Porphyromonas gingivalis* genes
44
45 conferring fitness in a tobacco-rich environment. Mol Oral Microbiol. 35(1):10-18.
46
47
48 Kigure T, Saito A, Seida K, Yamada S, Ishihara K, Okuda K. 1995. Distribution of
49
50 *Porphyromonas gingivalis* and *Treponema denticola* in human subgingival plaque at
51
52 different periodontal pocket depths examined by immunohistochemical methods. J
53
54 Periodontal Res. 30(5):332-341.
55
56
57
58
59
60

- 1
2
3 Kirst ME, Li EC, Alfant B, Chi YY, Walker C, Magnusson I, Wang GP. 2015. Dysbiosis and
4 alterations in predicted functions of the subgingival microbiome in chronic
5
6
7
8
9
10 Klein BA, Tenorio EL, Lazinski DW, Camilli A, Duncan MJ, Hu LDT. 2012. Identification
11
12
13
14
15
16
17 Lasica AM, Goulas T, Mizgalska D, Zhou X, de Diego I, Ksiazek M, Madej M, Guo Y,
18
19
20
21
22
23
24
25
26
27
28
29
30
31
32
33
34
35
36
37
38
39
40
41
42
43
44
45
46
47
48
49
50
51
52
53
54
55
56
57
58
59
60
- Lasica AM, Ksiazek M, Madej M, Potempa J. 2017. The type IX secretion system (T9SS):
Highlights and recent insights into its structure and function. *Front Cell Infect
Microbiol.* 7:215.
- Lauber F, Deme JC, Lea SM, Berks BC. 2018. Type 9 secretion system structures reveal a
new protein transport mechanism. *Nature.* 564(7734):77-82.
- Lenartova M, Tesinska B, Janatova T, Hrebicek O, Mysak J, Janata J, Najmanova L. 2021.
The oral microbiome in periodontal health. *Front Cell Infect Microbiol.* 11:629723.
- Ma H, Khan A, Nangia S. 2018. Dynamics of OmpF trimer formation in the bacterial outer
membrane of *Escherichia coli*. *Langmuir.* 34(19):5623-5634.
- Madej M, White JBR, Nowakowska Z, Rawson S, Scavenius C, Enghild JJ, Bereta GP,
Pothula K, Kleinekathoefer U, Basle A, et al. 2020. Structural and functional insights
into oligopeptide acquisition by the RagAB transporter from *Porphyromonas
gingivalis*. *Nat Microbiol.* 5(8):1016-1025.
- Madej M, Nowakowska Z, Ksiazek M, Lasica AM, Mizgalska D, Nowak M, Jacula A,
Bzowska M, Scavenius C, Enghild JJ, et al. 2021. PorZ, an essential component of the

1
2
3 type IX secretion system of *Porphyromonas gingivalis*, delivers anionic
4 lipopolysaccharide to the PorU sortase for transpeptidase processing of T9SS cargo
5 proteins. mBio. 12(1):e02262-02262.
6
7
8
9

10 Mark Welch JL, Dewhirst FE, Borisy GG. 2019. Biogeography of the oral microbiome: The
11 site-specialist hypothesis. Annu Rev Microbiol. 73:335-358.
12
13

14 Miller DP, Hutcherson JA, Wang Y, Nowakowska ZM, Potempa J, Yoder-Himes DR, Scott
15 DA, Whiteley M, Lamont RJ. 2017. Genes contributing to *Porphyromonas gingivalis*
16 fitness in abscess and epithelial cell colonization environments. Front Cell Infect
17 Microbiol. 7:378.
18
19
20
21
22

23 Moradali MF, Ghods S, Angelini TE, Davey ME. 2019. Amino acids as wetting agents:
24 surface translocation by *Porphyromonas gingivalis*. ISME J. 13(6):1560-1574.
25
26
27

28 Naito M, Tominaga T, Shoji M, Nakayama K. 2019. PGN_0297 is an essential component of
29 the type IX secretion system (T9SS) in *Porphyromonas gingivalis*: Tn-seq analysis
30 for exhaustive identification of T9SS-related genes. Microbiol Immunol. 63(1):11-20.
31
32
33
34

35 Nakane D, Sato K, Wada H, McBride MJ, Nakayama K. 2013. Helical flow of surface
36 protein required for bacterial gliding motility. Proc Natl Acad Sci U S A.
37
38
39
40
41
42

43 O'Brien-Simpson NM, Pathirana RD, Walker GD, Reynolds EC. 2009. *Porphyromonas*
44 *gingivalis* RgpA-Kgp proteinase-adhesin complexes penetrate gingival tissue and
45 induce proinflammatory cytokines or apoptosis in a concentration-dependent manner.
46
47
48
49
50
51

52 Paramonov N, Aduse-Opoku J, Hashim A, Rangarajan M, Curtis MA. 2015. Identification of
53 the linkage between A-polysaccharide and the core in the A-lipopolysaccharide of
54 *Porphyromonas gingivalis* W50. J Bacteriol. 197(10):1735-1746.
55
56
57
58
59
60

- 1
2
3 Rangarajan M, Aduse-Opoku J, Paramonov NA, Hashim A, Curtis MA. 2017. Hemin binding
4
5 by *Porphyromonas gingivalis* strains is dependent on the presence of A-LPS. Mol
6
7 Oral Microbiol. 32(5):365-374.
8
9
10 Roier S, Zingl FG, Cakar F, Durakovic S, Kohl P, Eichmann TO, Klug L, Gadermaier B,
11
12 Weinzerl K, Prassl R, et al. 2016. A novel mechanism for the biogenesis of outer
13
14 membrane vesicles in Gram-negative bacteria. Nat Commun. 7:10515.
15
16
17 Sato K, Naito M, Yukitake H, Hirakawa H, Shoji M, McBride MJ, Rhodes RG, Nakayama K.
18
19 2010. A protein secretion system linked to *Bacteroidete* gliding motility and
20
21 pathogenesis. Proc Natl Acad Sci U S A. 107(1):276-281.
22
23
24 Sato K, Okada K, Nakayama K, Imada K. 2020. PorM, a core component of bacterial type IX
25
26 secretion system, forms a dimer with a unique kinked-rod shape. Biochem Biophys
27
28 Res Commun. 532(1):114-119.
29
30
31 Schwechheimer C, Kuehn MJ. 2015. Outer-membrane vesicles from Gram-negative bacteria:
32
33 biogenesis and functions. Nat Rev Microbiol. 13(10):605-619.
34
35
36 Shi B, Lux R, Klokkevold P, Chang M, Barnard E, Haake S, Li H. 2020. The subgingival
37
38 microbiome associated with periodontitis in type 2 diabetes mellitus. ISME J.
39
40 14(2):519-530.
41
42
43 Shoji M, Sato K, Yukitake H, Kamaguchi A, Sasaki Y, Naito M, Nakayama K. 2018.
44
45 Identification of genes encoding glycosyltransferases involved in lipopolysaccharide
46
47 synthesis in *Porphyromonas gingivalis*. Mol Oral Microbiol. 33(1):68-80.
48
49
50 Smalley JW, Olczak T. 2017. Heme acquisition mechanisms of *Porphyromonas gingivalis* -
51
52 strategies used in a polymicrobial community in a heme-limited host environment.
53
54 Mol Oral Microbiol. 32(1):1-23.
55
56
57 Socransky SS, Haffajee AD, Cugini MA, Smith C, Kent RL, Jr. 1998. Microbial complexes
58
59 in subgingival plaque. J Clin Periodontol. 25(2):134-144.
60

- 1
2
3 Tan KH, Seers CA, Dashper SG, Mitchell HL, Pyke JS, Meuric V, Slakeski N, Cleal SM,
4
5 Chambers JL, McConville MJ, et al. 2014. *Porphyromonas gingivalis* and *Treponema*
6
7 *denticola* exhibit metabolic symbioses. PLoS Pathog. 10(3):e1003955.
8
9
10 Tompkins GR, Wood DP, Birchmeier KR. 1997. Detection and comparison of specific hemin
11
12 binding by *Porphyromonas gingivalis* and *Prevotella intermedia*. J Bacteriol.
13
14 179(3):620-626.
15
16
17 Tonetti MS, Jepsen S, Jin L, Otomo-Corgel J. 2017. Impact of the global burden of
18
19 periodontal diseases on health, nutrition and wellbeing of mankind: A call for global
20
21 action. J Clin Periodontol. 44(5):456-462.
22
23
24 Trinh NTT, Tran HQ, Van Dong Q, Cambillau C, Roussel A, Leone P. 2020. Crystal
25
26 structure of Type IX secretion system PorE C-terminal domain from *Porphyromonas*
27
28 *gingivalis* in complex with a peptidoglycan fragment. Sci Rep. 10(1):7384.
29
30
31 Veith PD, Chen YY, Gorasia DG, Chen D, Glew MD, O'Brien-Simpson NM, Cecil JD,
32
33 Holden JA, Reynolds EC. 2014. *Porphyromonas gingivalis* outer membrane vesicles
34
35 exclusively contain outer membrane and periplasmic proteins and carry a cargo
36
37 enriched with virulence factors. J Proteome Res. 13(5):2420-2432.
38
39
40 Veith PD, Glew MD, Gorasia DG, Reynolds EC. 2017. Type IX secretion: the generation of
41
42 bacterial cell surface coatings involved in virulence, gliding motility and the
43
44 degradation of complex biopolymers. Mol Microbiol. 106(1):35-53.
45
46
47 Veith PD, Luong C, Tan KH, Dashper SG, Reynolds EC. 2018. Outer membrane vesicle
48
49 proteome of *Porphyromonas gingivalis* is differentially modulated relative to the
50
51 outer membrane in response to heme availability. J Proteome Res. 17(7):2377-2389.
52
53
54 Veith PD, Shoji M, O'Hair RAJ, Leeming MG, Nie S, Glew MD, Reid GE, Nakayama K,
55
56 Reynolds EC. 2020. Type IX secretion system cargo proteins are glycosylated at the
57
58
59
60

1
2
3 C terminus with a novel linking sugar of the Wbp/Vim pathway. *Mbio*. 11(5):e01497-
4
5 01420.
6

7
8 Vincent MS, Canestrari MJ, Leone P, Stathopoulos J, Ize B, Zoued A, Cambillau C,
9
10 Kellenberger C, Roussel A, Cascales E. 2017. Characterization of the *Porphyromonas*
11
12 *gingivalis* type IX secretion trans-envelope PorKLMNP core complex. *J Biol Chem*.
13
14 292(8):3252-3261.
15
16

17 Vincent MS, Chabalier M, Cascales E. 2018. A conserved motif of *Porphyromonas* Type IX
18
19 secretion effectors C-terminal secretion signal specifies interactions with the
20
21 PorKLMN core complex. *bioRxiv*. doi: <https://doi.org/10.1101/483123>.
22
23

24 Yukitake H, Shoji M, Sato K, Handa Y, Naito M, Imada K, Nakayama K. 2020. PorA, a
25
26 conserved C-terminal domain-containing protein, impacts the PorXY-SigP signaling
27
28 of the type IX secretion system. *Sci Rep*. 10(1):21109.
29

30 Zhang Z, Liu D, Liu S, Zhang S, Pan Y. 2020. The role of *Porphyromonas gingivalis* outer
31
32 membrane vesicles in periodontal disease and related systemic diseases. *Front Cell*
33
34 *Infect Microbiol*. 10:585917.
35
36
37
38
39
40
41
42
43
44
45
46
47
48
49
50
51
52
53
54
55
56
57
58
59
60

FIGURE LEGENDS

Figure 1: Multiple PorL/M motors form a funnel-shaped cage in the periplasm

Cross-section of the trans-envelope complex showing half of a PorK/N ring in the outer membrane (OM) and a small number of PorL/M motors in the inner membrane (IM). The pentameric PorL stator is shown in blue and encloses the two trans-membrane helices of the PorM dimer (one from each monomer). The PorM shaft is composed of four periplasmic domains shown in green. Considering the abundance of PorKLMN proteins relative to each other in whole cells, the number of PorM molecules should be similar to the number of PorK and PorN molecules which is estimated to be 32-36 per ring based on cryo-EM images (Gorasia et al. 2016). Since there are only two PorM molecules per motor complex, we predict that many motors (possibly 16-18 of them) form a ring in the IM with their bent shafts forming a dynamic funnel-shaped cage in the periplasm. One PorW subunit forms a bridge to the single translocon (Sov) which is shown bound to the PorV shuttle protein (Gorasia et al. 2020a).

Figure 2: Proposed cargo delivery from PorM to PorV

The spatial organization of the T9SS ((Gorasia et al. 2020a) and unpublished) together with data showing that the CTD signals of cargo proteins interact with PorM, PorN and PorW ((Vincent et al. 2018) and unpublished) suggest a pathway for the delivery of cargo to the secretion pore. The cargo (pink) are recruited by the rotating shafts of PorM (green) and passed to PorN (yellow). PorN is proposed to physically move along the PorK track (grey) transporting the cargo with it. At one point along the circular track, the cargo is passed to PorW (orange) and then to the Sov translocon (blue). The cargo is secreted through Sov and delivered to the PorV shuttle protein (green). Note that the track is shown as a straight block since it has not yet been determined whether Sov and PorV are on the inside or outside of the ring.

Figure 3. Proposed mechanism and pathway of cargo delivery to the attachment complexes

1
2
3 The delivery of cargo from the translocon (Sov) to the attachment complex comprised of
4 PorU, PorV, PorZ and PorQ is an outstanding question of considerable interest. This figure is
5 a speculative model that assumes that this process occurs outside of the PorK/N rings (A)
6 Once secreted and bound to PorV, the cargo (pink) are proposed to be passed along a series
7 of PorV molecules until they reach an attachment complex where they are processed to
8 become permanently attached to the OM via conjugation to A-LPS. The PorV chain may be
9 continuous (as depicted) or it may have gaps requiring short diffusion distances to be
10 covered. In this latter case, the PorV-PorV interactions may be dynamic. (B) In the context of
11 a whole cell, we envisage a tree-like arrangement of PorV highways that connect a small
12 number of translocation systems to a much larger number of attachment complexes at a ratio
13 of approximately 1:8 (Glew et al. 2017). The major outer membrane proteins of Gram-
14 negative bacteria are known to be organized into “Omp islands” which are areas of extremely
15 low diffusion (Chavent et al. 2018). The T9SS shuttle system would be located outside of
16 these areas where there is higher diffusion and where the OM has more freedom to bulge out
17 and form OMVs.

18
19
20
21
22
23
24
25
26
27
28
29
30
31
32 **Figure 4. A working model of pathogenic mechanisms mediated by OMVs loaded with**
33 **virulence factors secreted by the T9SS**

34
35
36 *P. gingivalis* secretes and attaches cargo proteins to A-LPS to form a virulent coat on the
37 surface of the cell using the T9SS. The two-component system, PorY and PorX, activate the
38 SigP sigma factor to control the expression of many T9SS related genes. The cargo proteins
39 are first secreted through the Sec translocon via their N-terminal leader sequence, then are
40 transported to Sov via CTD binding to various PorM domains followed by binding to PorW
41 which anchors Sov to the PorN-PorK ring. This transport requires the proton motive force
42 harnessed by the IM helices of PorL and PorM forming the motor. Removal of the plug from
43 Sov allows the CTD of the cargo protein to enter the exposed periplasmic Sov opening where
44 it binds to surface loop(s) of docked PorV at the external-side Sov opening. The CTD-cargo
45 protein bound to PorV is released to the surface and is delivered to the attachment complex
46 where PorU cleaves off the CTD and covalently links the new C-terminus via
47 transpeptidation to the 2-N-seryl-3-N-acetylglucuronamide of A-LPS that is recruited by
48 PorZ. PorU and PorZ are anchored to the OM by PorQ and PorV respectively. Due to
49 environmental signals, such as iron-limitation, these secreted cargo proteins are then
50
51
52
53
54
55
56
57
58
59
60

1
2
3 packaged into OMVs which are released into the surroundings where they can act at a
4 considerable distance from the source cell. *P. gingivalis* can interact antagonistically toward
5 some bacteria, for example through the disruption of oral streptococcal biofilms by
6 gingipains enriched on the surface of OMVs. The μ -oxo bisheme is extracted from the host
7 through the action of surface gingipains on cells and OMVs and stored on the surface by
8 binding to A-LPS. The heme-loaded OMVs can then disperse to synergistically promote the
9 growth of other subgingival microbiota, via fusion with their outer membranes and exchange
10 of hemin bound A-LPS. This alters the oral microbiota and proportion of virulence factors to
11 cooperatively promote disease: By disrupting the epithelial barrier due to degradation of the
12 tight junctions between host cells, increasing host cell invasion and causing dysbiosis of host
13 systems ultimately leading to chronic inflammation and the destruction of the tooth
14 supporting tissues including bone. Structures for Plug (red, PDB ID: 6H3J) and Sov_PorV
15 (blue_light green, PDB ID: 6H3I) complexes, and the PorM-PorL motor (hot
16 pink+cornflower blue_purple, PDB ID: 6ys8) were determined by cryo-EM (Hennell James
17 et al. 2021; Lauber et al. 2018). The crystal structures for mature RgpB (PDB ID: 1CVR) and
18 RgpB CTD (PDB ID: 5AG9) were used for the cargo proteins. PorZ (purple) and PorM dimer
19 (hot pink+cornflower blue) were from crystal structures (PDB ID: 5m11 (Lasica et al. 2016)
20 and PDB ID: 7cmg (Sato et al. 2020), respectively). PorG (dark green), PorP (medium blue),
21 PorV (light green) and PorQ (magenta) β -barrel structures are from Phyre2 models using
22 amino acid sequences without N-terminal signal peptides. The PorU structure is a Phyre2
23 model without a signal peptide or domain A (Glew et al. 2012). Attachment and cargo shuttle
24 complexes are depicted based on composition of complexes and subcomplexes (Glew et al.
25 2017).

26
27
28
29
30
31
32
33
34
35
36
37
38
39
40
41
42
43
44
45
46
47
48
49
50
51
52
53
54
55
56
57
58
59
60

Table 1. T9SS-related genes that are essential for growth or fitness identified by TnSeq

| Gene Name | 33277 Locus Tag | W83 Locus Tag | Ortholog in <i>Pi</i> or <i>Tf</i> | Protein Description | Inherently Essential for Growth ^a | Essential for Fitness ^b |
|---------------------------|-----------------|---------------|------------------------------------|--|--|------------------------------------|
| T9SS components | | | | | | |
| <i>plug</i> | PGN_0144 | PG2092 | <i>Pi, Tf</i> | Plugs periplasmic opening of Sov | - | - |
| <i>porA^{c,d}</i> | PGN_0123 | PG2172 | -, - | Proposed T9SS regulatory signal receptor | - | - |
| <i>porE</i> | PGN_1296 | PG1058 | <i>Pi, Tf</i> | PorP-associated lipoprotein; peptidoglycan binding domain | + | - |
| <i>porF</i> | PGN_1437 | PG0534 | <i>Pi, Tf</i> | Predicted TonB-dependent receptor | + | - |
| <i>porG</i> | PGN_0297 | PG0189 | <i>Pi, Tf</i> | Predicted 8-stranded OM β -barrel associated with PorK/N | + | - |
| <i>porK</i> | PGN_1676 | PG0288 | <i>Pi, Tf</i> | OM lipoprotein, forms large periplasmic rings with PorN | - | - |
| <i>porL</i> | PGN_1675 | PG0289 | <i>Pi, Tf</i> | Motor stator | + | - |
| <i>porM</i> | PGN_1674 | PG0290 | <i>Pi, Tf</i> | Motor rotor and shaft | + | - |
| <i>porN</i> | PGN_1673 | PG0291 | <i>Pi, Tf</i> | Forms large periplasmic rings in association with PorK | + | - |
| <i>porP</i> | PGN_1677 | PG0287 | <i>Pi, Tf</i> | Predicted 14-stranded OM β -barrel, binds to PorE. | + | - |
| <i>porQ</i> | PGN_0645 | PG0602 | <i>Pi, Tf</i> | Attachment complex, 14-stranded OM β -barrel, binds to PorZ | + | - |
| <i>porT</i> | PGN_0778 | PG0751 | <i>Pi, Tf</i> | Predicted 8-stranded OM β -barrel protein | - | - |
| <i>porU^c</i> | PGN_0022 | PG0026 | <i>Pi, Tf</i> | Attachment complex, T9SS sortase, binds to PorV | + | - |
| <i>porV</i> | PGN_0023 | PG0027 | <i>Pi, Tf</i> | T9SS shuttle protein and attachment complex member, 14-stranded OM β -barrel, binds to PorU, Sov, PorA and other cargo | + | - |
| <i>porW</i> | PGN_1877 | PG1947 | <i>Pi, Tf</i> | OM lipoprotein, forms bridge between PorN and Sov | - | - |
| <i>porX</i> | PGN_1019 | PG0928 | <i>Pi, Tf</i> | Two-component response regulator, activates SigP | + | - |
| <i>porY</i> | PGN_2001 | PG0052 | <i>Pi, Tf</i> | Two-component histidine kinase, activates PorX | + | - |
| <i>porZ^{c,d}</i> | PGN_0509 | PG1604 | <i>Pi, Tf</i> | Attachment complex, binds to PorQ, and A-LPS. | - | - |
| <i>sigP</i> | PGN_0274 | PG0162 | <i>Pi, Tf</i> | Extracytoplasmic function sigma factor, σ^P | - | - |
| <i>sov</i> | PGN_0832 | PG0809 | <i>Pi, Tf</i> | T9SS translocon, gated by its binding to PorV or Plug | + | - |
| A-LPS biosynthesis | | | | | | |
| <i>ugdA</i> | PGN_0613 | PG1277 | <i>Pi, Tf</i> | UDP-D-GlcNAc 6-dehydrogenase | + | E, M |
| <i>wbpA</i> | PGN_1243 | PG1143 | <i>Pi, Tf</i> | UDP-D-GlcNAc 6-dehydrogenase | + | E, M |
| <i>wbpB</i> | PGN_0168 | PG2119 | -, <i>Tf</i> | C3-dehydrogenase | - | E, M, C |
| <i>wbpD</i> | PGN_0002 | PG0002 | -, <i>Tf</i> | Acetyltransferase | - | E, M, C |
| <i>wbpE</i> | PGN_1236 | PG1138 | <i>Pi, Tf</i> | Aminotransferase | - | - |
| <i>wbpS</i> | PGN_1234 | PG1136 | -, - | Amidotransferase | + | - |
| <i>vimE</i> | PGN_1055 | PG0883 | -, <i>Tf</i> | Deacetylase | - | - |

| | | | | | | | |
|----|-------------------|----------|--------|---------------|---|---|---------|
| 1 | <i>vimA</i> | PGN_1056 | PG0882 | -, <i>Tf</i> | N-seryltransferase | - | - |
| 2 | <i>wbaP</i> | PGN_1896 | PG1964 | <i>Pi, Tf</i> | Phosphoglycosyltransferase, putative transfer of first sugar of A-LPS repeating unit. | + | - |
| 3 | | | | | | | |
| 4 | <i>gtfC</i> | PGN_0242 | PG0129 | <i>Pi, Tf</i> | Putative rhamnosyltransferase | + | E, M |
| 5 | <i>gtfF</i> | PGN_1668 | PG0294 | <i>Pi, -</i> | Glycosyltransferase family 2 | + | - |
| 6 | <i>vimF</i> | PGN_1054 | PG0884 | -, <i>Tf</i> | Glycosyltransferase family 2, putative transfer of linking sugar | + | - |
| 7 | | | | | | | |
| 8 | | | | | | | |
| 9 | | | | | | | |
| 10 | | | | | | | |
| 11 | T9SS cargo | | | | | | |
| 12 | <i>tapA</i> | PGN_0152 | PG2102 | | TprA-associated protein, mutant is less virulent in murine lesion model | - | E, M |
| 13 | | | | | | | |
| 14 | <i>mfa5</i> | PGN_0291 | PG0182 | | Tip fimbrillin of MfaI fimbriae, mutation reduces MfaI fimbriae abundance | - | E, C |
| 15 | | | | | | | |
| 16 | <i>cpg70</i> | PGN_0335 | PG0232 | | Metalloprotease, processes gingipains, mutant less virulent in murine lesion model | - | E, C |
| 17 | | | | | | | |
| 18 | | | | | | | |
| 19 | | | | | | | |
| 20 | <i>prtT</i> | PGN_0561 | PG1548 | | Thiol protease related to periodontain | - | E, M, C |
| 21 | | PGN_0654 | PG0611 | | Function unknown | - | E, M |
| 22 | | PGN_0657 | PG0614 | | Function unknown | - | - |
| 23 | | | | | | | |
| 24 | <i>hbp35</i> | PGN_0659 | PG0616 | | Hemin binding protein with multiple virulence properties | - | - |
| 25 | | | | | | | |
| 26 | | PGN_0693 | PG0654 | | Function unknown | + | - |
| 27 | | PGN_0795 | PG0769 | | Function unknown | - | E, M, C |
| 28 | | PGN_0852 | PG1374 | | Leucine-rich repeat protein | - | E, M, C |
| 29 | | | | | | | |
| 30 | <i>ppaD</i> | PGN_0898 | PG1424 | | Peptidylarginine deiminase, role in rheumatoid arthritis | + | E, M, C |
| 31 | | | | | | | |
| 32 | <i>prtT</i> | PGN_0900 | PG1427 | | Periodontain, thiol protease and haemagglutinin, rapidly inactivates α_1 -proteinase inhibitor of neutrophil elastase | - | E, M, C |
| 33 | | | | | | | |
| 34 | | | | | | | |
| 35 | | PGN_1115 | PG1326 | | Haemagglutinin | - | - |
| 36 | | PGN_1321 | PG1030 | | Function unknown | + | E, M, C |
| 37 | | | | | | | |
| 38 | <i>pepK</i> | PGN_1416 | PG0553 | | Lys-specific serine endopeptidase | - | E, M, C |
| 39 | | | | | | | |
| 40 | <i>rgpB</i> | PGN_1466 | PG0506 | | Arg-specific gingipain (cysteine proteinase), multiple virulence properties, less virulent in multiple animal models of disease | - | E, M, C |
| 41 | | | | | | | |
| 42 | | | | | | | |
| 43 | | PGN_1476 | PG0495 | | Function unknown | + | E, M |
| 44 | | PGN_1556 | PG0411 | | Haemagglutinin | - | E, M |
| 45 | <i>inlJ</i> | PGN_1611 | PG0350 | | Internalin, leucine-rich repeat protein, role in homotypic and heterotypic biofilm formation and epithelial cell invasion | - | E, M |
| 46 | | | | | | | |
| 47 | | | | | | | |
| 48 | <i>kgp</i> | PGN_1728 | PG1844 | | Lys-specific gingipain (cysteine proteinase), multiple virulence properties, less virulent in multiple animal models of disease | - | - |
| 49 | | | | | | | |
| 50 | | | | | | | |
| 51 | <i>hagA</i> | PGN_1733 | PG1837 | | Haemagglutinin | - | E, M |
| 52 | | PGN_1767 | PG1798 | | Function unknown | - | - |
| 53 | | PGN_1770 | PG1795 | | Function unknown | + | E, M |
| 54 | | | | | | | |
| 55 | <i>rgpA</i> | PGN_1970 | PG2024 | | Arg-specific gingipain (cysteine proteinase), multiple virulence properties, less virulent in multiple animal models of disease | - | E, M |
| 56 | | | | | | | |
| 57 | | | | | | | |
| 58 | | PGN_2065 | PG2198 | | Function unknown | - | E, M |
| 59 | | PGN_2080 | PG2216 | | Function unknown | + | E, M |
| 60 | | | | | | | |

1 ^aFound to be inherently essential in at least one of three TnSeq studies (Hutcherson et al. 2016; Klein et al. 2012; Miller et al. 2017).

2 ^bFound to be conditionally essential and required under defined conditions: Epithelial colonization (E), murine abscess formation
3 (M), cigarette smoke extract exposure (C) (Hutcherson et al. 2020; Miller et al. 2017).

4 ^cCodes for a protein that is both a T9SS component and a cargo protein.

5 ^dNo sequence detected in TnSeq output pool of one to two conditions tested for fitness.

6 GlcNAc, N-acetyl-D-glucosamine;

7
8
9
10
11
12
13
14
15
16
17
18
19
20
21
22
23
24
25
26
27
28
29
30
31
32
33
34
35
36
37
38
39
40
41
42
43
44
45
46
47
48
49
50
51
52
53
54
55
56
57
58
59
60

For Peer Review

1
2
3
4
5
6
7
8
9
10
11
12
13
14
15
16
17
18
19
20
21
22
23
24
25
26
27
28
29
30
31
32
33
34
35
36
37
38
39
40
41
42
43
44
45
46
47
48
49
50
51
52
53
54
55
56
57
58
59
60

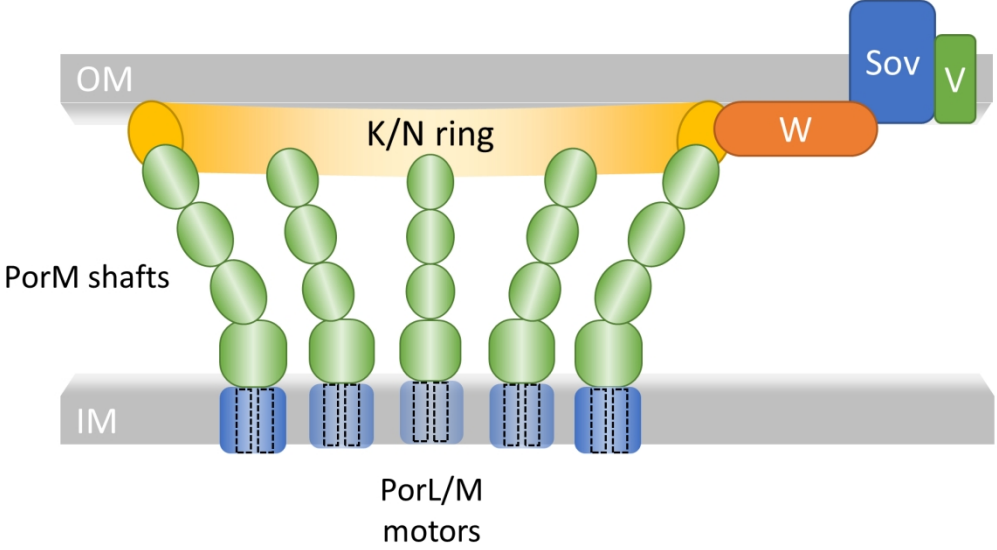


Figure 1: Multiple PorL/M motors form a funnel-shaped cage in the periplasm

165x91mm (300 x 300 DPI)

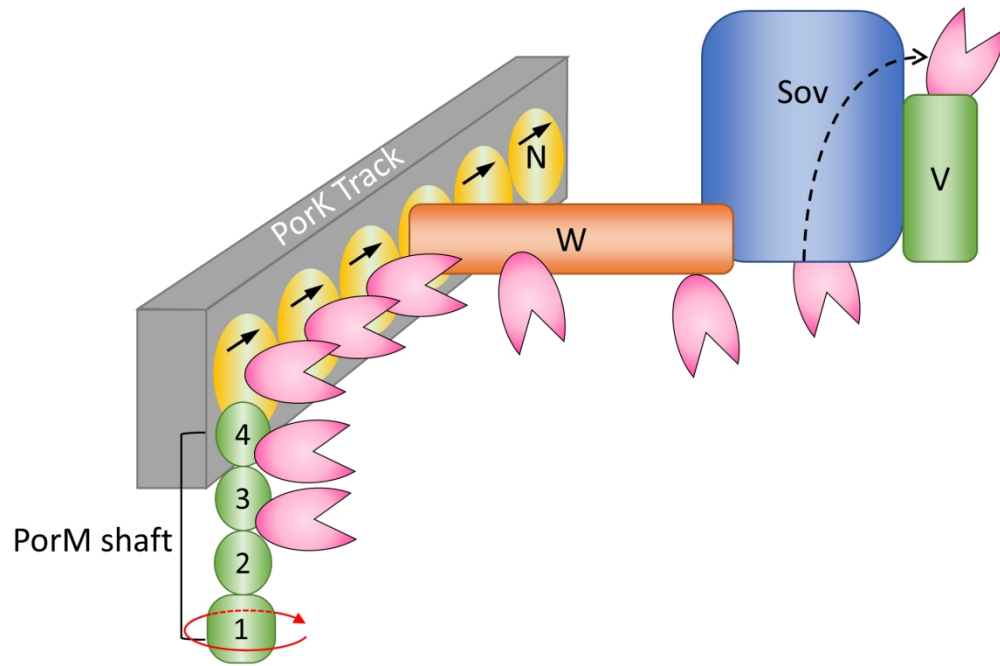


Figure 2: Proposed cargo delivery from PorM to PorV

176x118mm (300 x 300 DPI)

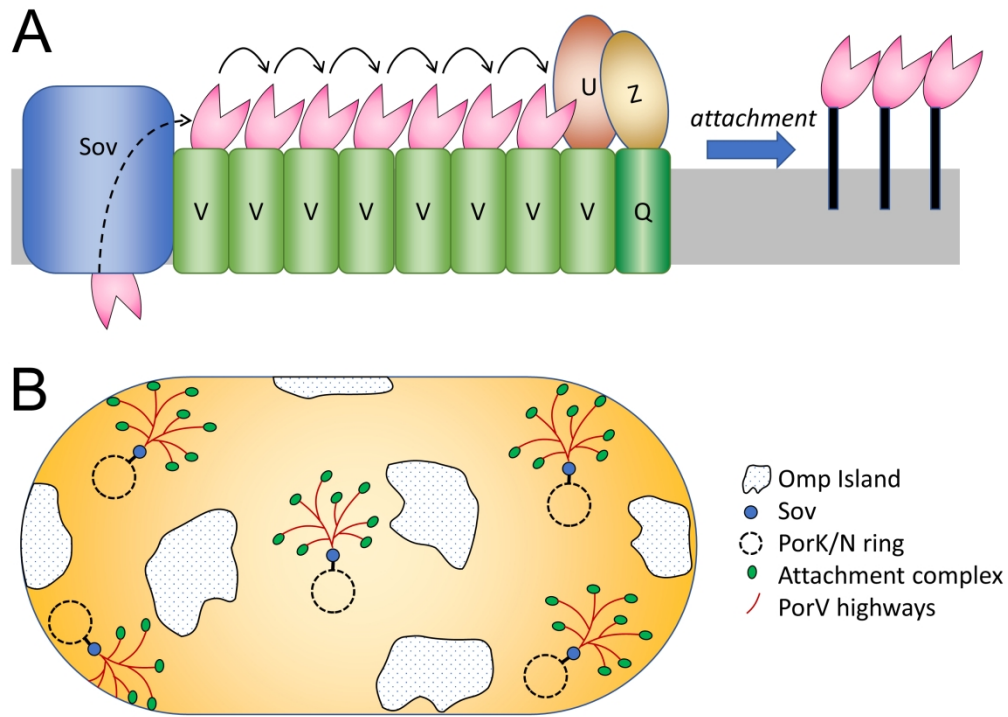


Figure 3. Proposed mechanism and pathway of cargo delivery to the attachment complexes.

236x169mm (300 x 300 DPI)

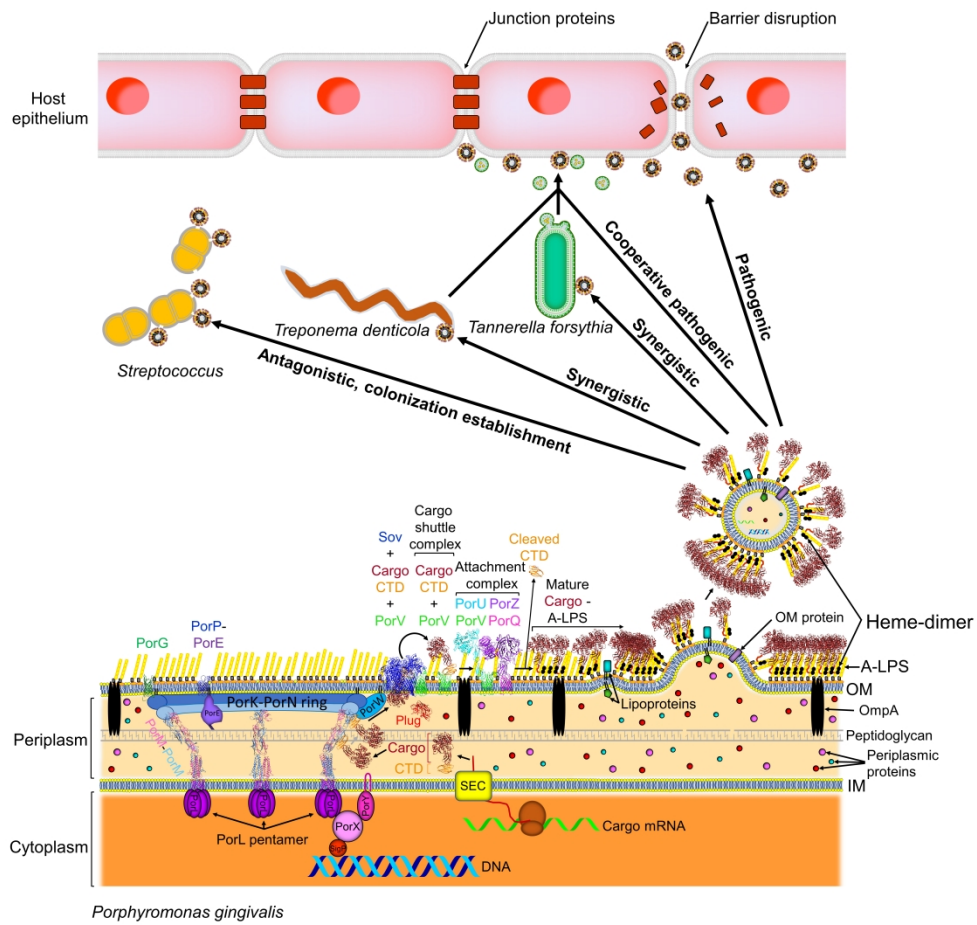


Figure 4. A working model of pathogenic mechanisms mediated by OMVs loaded with virulence factors secreted by the T9SS.

506x506mm (300 x 300 DPI)